Q. J. R. Meteorol. Soc. (2006), **132**, pp. 2749–2768 doi: 10.1256/qj.05.185

The surface energy balance and boundary layer over urban street canyons

By I. N. HARMAN* and S. E. BELCHER
University of Reading, UK

(Received 31 August 2005; revised 14 July 2006)

SUMMARY

A model is developed for the energy balance of an urban area, represented as a sequence of two-dimensional street canyons. The model incorporates a novel formulation for the sensible-heat flux, that has previously been validated against wind tunnel models, and a formulation for radiation that includes multiple reflections and shadowing. This energy balance model is coupled to a model for the atmospheric boundary layer. Results are analysed to establish how the physical processes combine to produce the observed features of urban climate, and to establish the roles of building form and fabric on the urban modification to climate.

Over a diurnal cycle there are morning and evening transition periods when the net flux of radiation is largely balanced by the flux of heat into the surface. The urban surface has a large surface area in contact with the air, and hence a large active heat capacity, and so the urban area needs to absorb a larger amount of heat than a rural area to change the surface temperature. The morning and evening transitions are therefore prolonged over urban areas, delaying the onset of convective or stable boundary layers after sunrise and sunset. The model shows that the energy balance of the roof behaves very differently from the combined energy balance of the street canyon system of walls and street. The sensible-heat flux from the street canyon into the boundary layer is increased by the increased surface area, but is decreased by the buildings reducing the local flow speeds. The net result is that, for the two-dimensional geometry investigated here, the sensible-heat flux from the canyon is not strongly sensitive to canyon geometry. The sensible-heat flux from the roof is larger than from the street, and so the total sensible-heat flux into the boundary layer, and hence also the air temperature, is strongly dependent on the fraction of plan area occupied by roofs. The radiation budget of the street canyon, which largely drives the temperatures of the canyon surfaces, is significantly changed by the limited sky view and multiple reflections caused by the local building form. The canyon surface temperatures thus depend strongly on local building morphology.

Finally, two mechanisms are suggested for how urban areas might maintain a positive sensible-heat flux at night. Firstly, if the roof material has much lower heat capacity than the street canyon surfaces, then the roof can cool the boundary-layer air faster than the street canyon surfaces cool, leading to a positive heat flux out of the street canyon. Secondly, advection decouples the boundary layer from the local surface energy balance. In this way, cool air, perhaps from a rural area, advected on to an urban surface can lead to a positive sensible-heat flux which then tends to neutralize any stable stratification in the boundary layer.

KEYWORDS: Urban energy balance Urban heat island Urban meteorology

1. INTRODUCTION

There are many applications that require an understanding or predictive capability of the local climate and weather in urban areas. These include the parametrization of urban areas into numerical weather prediction (NWP) models (see Dabberdt *et al.* 2000 for a recent review of requirements), air-quality forecasting (see Dabberdt *et al.* 2004) and energy demand forecasting for buildings, particularly as the climate warms (Hacker *et al.* 2005). Urban areas change the local climate by altering the thermodynamics of the surface energy balance and its coupling with the boundary layer above. But, as the reviews by Oke (1982) and more recently Arnfield (2003) demonstrate, there is a bewildering range of possible physical mechanisms effecting the changes, many of which remain to be quantified. Observations suggest that, whilst there is variability between different urban areas, there are generic features of the impacts upon the local climate, which suggests that amongst the myriad of physical processes a subset dominates. We review briefly these generic features in section 2.

With the recent move to higher resolution in NWP, there has been much research recently into the urban energy balance, leading to a number of quantitative models based

* Corresponding author, current affiliation: CSIRO Marine and Atmospheric Research, GPO Box 1666, Canberra 2601, Australia. e-mail: ian.harman@csiro.au

on physical processes, see for example Masson (2000), Martilli *et al.* (2002) and Best (2005). These models differ in conception and in complexity, but at this time there is no consensus over the level of detail required in the modelling for different applications. Furthermore, it is unclear how these energy balance models work to control the fluxes in the energy balance: to what extent is the energy balance controlled by the fabric of the buildings, and to what extent it is controlled by the geometric form of the buildings?

Here we address these questions by developing an energy balance model for a two-dimensional street canyon as an idealization of an urban area. Studies over vegetated surfaces (e.g. McNaughton and Spriggs 1986) show that there is tight coupling between the surface energy balance and the boundary layer. For this reason, the urban energy balance model is then coupled to a model for the atmospheric boundary layer. We then analyse in detail results of the model to determine both how the dominant physical processes balance, and the extent to which it explains the generic features observed in urban areas. This is an important step because it helps to show how the physical parameters of the simplified model combine to produce the climatic features of urban areas. Hence the answers to these questions will inform the choice of input parameters to be used in the simple model to represent a real complex urban geometry.

We first review in section 2 the challenges and current understanding of the urban energy balance–boundary layer system. Section 3 gives an overview of the modelling tools used in this paper. Section 4 considers the idealized diurnal cycle of the surface energy balance and boundary layer over flat and urban surfaces and identifies the processes that give rise to the differences. Section 5 describes how the temperatures of the surfaces and of the boundary-layer air evolve in the coupled system. Section 6 then illustrates some of the sensitivities of the model, with a particular focus on the nocturnal energy balance. Finally, we end in section 7 with conclusions.

2. Characteristics of the urban climate

Schmid *et al.* (1991) show how measurements of scalar fluxes have high spatial variability across urban areas, due to the high spatial variability in building fabric and form and in land use across urban areas. Nevertheless, observations of the urban energy balance and boundary layer (e.g. Grimmond and Oke 1995, 2002), and particularly those that also report simultaneous measurements from a rural location (Cleugh and Oke 1986; Grimmond *et al.* 1993; Christen and Vogt 2004), yield evidence of generic characteristics of urban areas:

(i) Momentum flux: Urban areas are typically aerodynamically rougher than the rural surroundings (e.g. Oke 1987).

(ii) Latent-heat flux: Typically smaller in urban areas than the rural surroundings (e.g. Cleugh and Oke 1986).

(iii) Sensible-heat flux: Urban areas generally have a larger sensible-heat flux than rural surroundings and can maintain a positive sensible-heat flux throughout the night (e.g. Oke *et al.* 1999).

(iv) Ground heat flux/storage: During the day the heat flux into the urban fabric is larger than the ground heat flux in rural surroundings; this energy stored in the building fabric can then be released to the atmosphere at night (e.g. Cleugh and Oke 1986).

(v) Anthropogenic heat fluxes: May play a significant role in some cities (e.g. Ichinose *et al.* 1999).

(vi) Surface energy balance: Urban areas change the phasing of the terms of the surface energy balance. The ground heat/storage term often peaks earlier and the sensible-heat flux often peaks later than in rural areas (e.g. Grimmond and Oke 2002).

(vii) Urban temperatures: The urban surface, urban canopy air, and overlying boundary layer are commonly warmer than the rural counterparts during the night. These are the well-known *urban heat islands* (e.g. Oke 1987).

(iix) Boundary-layer structure: The urban boundary layer often shows similar characteristics to the surrounding rural boundary layer during the day. The tendency for positive sensible-heat flux at night in urban areas leads to a nearly neutral temperature profile at night when the surrounding rural area becomes stably stratified (Oke and East 1971).

The features of urban areas that lead to these characteristics can be divided into three categories:

(i) Building fabric: The fabric of a surface has many important properties including the albedo and emissivity, heat capacity, thermal conductivity and the surface roughness. These material properties are all likely to be different from rural areas, and thus change the magnitude of the fluxes in the urban energy balance.

(ii) Building form: The geometrical form of the urban surface changes the fluxes in the urban energy balance in several ways:

(a) The geometry of the surface changes further the radiative terms of the energy balance. Shadowing leads to variation in the direct solar radiation incident on different building facets. Outgoing long-wave radiation from one facet may be absorbed by another facet, with only a fraction being lost to the sky. This effect of limited *sky view*, plays an important role in establishing nocturnal surface heat islands (Oke 1981; Oke *et al.* 1991).

(b) Building form also changes the airflow within the urban canopy in the boundary layer. The buildings act as bluff bodies which remove momentum from the airflow through pressure drag, thereby reducing the spatially averaged mean wind speeds according to the density of buildings (MacDonald *et al.* 1998; Belcher *et al.* 2003; Coceal and Belcher 2004). The geometrical form of the buildings creates patterns of non-uniform flow adjacent to the building facets, which then control the local turbulent transport of scalar. Since these local motions scale on the mean spatially averaged wind speed, the result is a tendency to reduce turbulent transport from the building surfaces (Harman *et al.* 2004b).

(c) The area of urban surface in contact with air, per unit plan area of ground, is larger than for a flat surface. A greater surface area is then available for energy exchange with the atmosphere. The flux of direct solar radiation tends to be shared amongst a larger surface area of building facets. The increase in total surface area increases the sensible-heat flux per unit plan area. This increase is, however, offset by the reduced efficiency of turbulent transport described in the previous point.

(iii) Anthropogenic factors: Anthropogenic factors can be direct, such as the output of heat from chimneys or exhausts, or indirect, such as enhanced mixing due to traffic generated turbulence. Water control, for instance the use of waterproofing, efficient drainage or irrigation within urban areas affects the energy balance by controlling the availability of water for evaporation and thence latent-heat fluxes (e.g. Grimmond *et al.* 1993). Finally, aerosols, largely anthropogenically produced, change radiative transfer and may alter the radiative fluxes at the surface (Oke 1982).

What controls the magnitudes of these different characteristics and how do they interact? Arnfield and Grimmond (1998) and Grimmond and Oke (1999) have highlighted the role played by the ground heat flux and storage of heat in the urban fabric.

Oke *et al.* (1991) considered the cooling rate of an idealized urban surface in the absence of turbulent heat transport. The effects of building morphology on the exchange of long-wave radiation was shown to be the principal control on the evolution of the surface temperature, with the thermal admittance of the building material being of second-most importance. Barlow and Belcher (2002) and Barlow *et al.* (2004) show that the turbulent transfer from an urban surface has a complex dependency on the surface form. Mills and Arnfield (1993) and Masson (2000) show complex relationships between the net energy balance of the urban surface and the energy balances of the individual building facets. It is therefore not surprising that, while night-time surface temperature anomalies correlate well with the local building form, the more ubiquitous urban canopy heat islands correlate less significantly (Bärring *et al.* 1985). These process studies have shown the role of different processes in isolation. However, few of these models have been used to systematically investigate the physical processes occurring in urban areas and how they interact. Such knowledge is needed in the development of surface exchange parametrization schemes within NWP (e.g. Masson 2000; Martilli *et al.* 2002; Best 2005). Finally, if a simple street canyon model is to be used to represent the complexity of a real urban geometry, how should the physical parameters of the simple model be chosen? Good understanding of the physical processes represented in the simple model is essential.

With these motivations in mind, we seek in this paper to determine the impacts of building fabric and form on the coupled energy balance–boundary layer system. This is done here by examining the results of a coupled energy balance–boundary layer model. The energy balance is a reasonably complete representation of a simplified two-dimensional street canyon system. In the spirit of the motivation of getting basic understanding of an idealized system, moisture is ignored completely. (Within an NWP framework moisture fluxes could be handled through a tiled approach.) Our aim here is to get understanding that can subsequently be used to help formulate a strategy for selecting parameters for the simplified model in order to represent real urban geometry and thence to compare the model with observations.

3. Model Description

The model consists of three components: a model for heat transport in the substrate of the building material and ground surface; the thermodynamics and dynamics of the atmospheric boundary layer; the energy balance of the roughness sublayer, which mediates energy exchange between the ground surface and the atmospheric boundary layer. The division into these three components is shown schematically in Fig. 1.

The substrate ranges from the building surface or ground surface, where there is an interface with the atmosphere, downwards into the earth. The surface energy balance is here defined to be the energy balance of the volume of air from the building or ground surface up to a horizontal level, z_*, where turbulence has mixed fluxes so that they are horizontally homogeneous (*the top of the roughness sublayer*, see Rotach (1999); cf. the blending height described by Mason 1988). Such a level is possible to define because we use a periodically repeating urban geometry, namely the urban street canyon (e.g. Oke *et al.* 1991). Hence, through the volume of the *roughness sublayer* the non-uniform fluxes from the different facets of the urban surface are mixed into a homogeneous flux that drives the evolution of the boundary layer above. The boundary layer is the layer of air from z_* upwards that is mixed by turbulence, here up to a temperature inversion. Since the boundary layer is driven by *spatially* homogeneous fluxes its properties vary only with height.

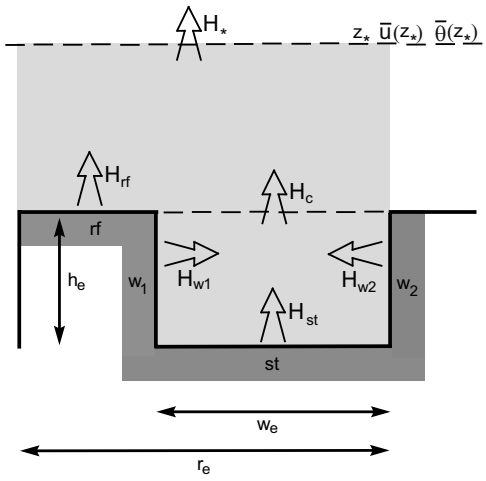

Figure 1. Perspective schematic of an urban street canyon and the characteristic dimensions and nomenclature used. The urban street canyon comprises infinitely long, parallel, uniform buildings with flat roofs; h_e, w_e and r_e stand for the height, separation width and repeating width of the building elements and are used to avoid confusion with H representing the sensible-heat flux density or h representing the height of the boundary layer. The four facets of the urban street canyon are the street (st), the two walls (w_1 and w_2) and the roof (rf). The three components are the boundary-layer model (above the reference level z_*), the roughness sublayer (light shading) and the building fabric (dark shading). $H_* = \rho c_p u_* \theta_*$ is the value of the (spatially homogeneous) sensible-heat flux density at the reference level, where ρ is air density, c_p is the heat capacity of air at constant pressure, u_* is the friction velocity and θ_* the scale of the fluctuations in potential temperature. In practice z_* is taken to be twice the height of the building and is the lowest level on which we calculate the mean wind speed $\overline{U}$ and potential temperature $\overline{\theta}$.

The energy balance at z_* is the composite of the energy balances of the four facets of the two-dimensional street canyon. We construct the energy balance for each of these facets by considering the facet-averaged temperature profile within the substrate of the facet as described in the following subsections.

The main novelties of the model are the treatment of the radiation physics, in particular the reflections, and in the treatment of the sensible-heat flux. We also show that coupling between the energy balance and the boundary-layer dynamics places important constraints on the evolution of the urban climate.

(*a*) *Heat transport in the substrate*

We consider the heat transport in each of the four facets of the urban street canyon separately. Heat transport normal to the surface is assumed larger than transport parallel, which is therefore neglected. The heat transport within each facet can therefore be formulated in terms of the substrate temperature profile T. The evolution of T within a stratified substrate experiencing homogeneous forcing is given by Eq. (1), where C_s and k are the volumetric heat capacity and thermal conductivity of the substrate, respectively, G is the ground heat flux density, and n is the co-ordinate normal to the surface with $n = 0$ at the surface and decreasing into the substrate:

$$C_s \frac{dT}{dt} = \frac{dG}{dn}, \tag{1a}$$

$$G = k \frac{dT}{dn}. \tag{1b}$$

Equations (1a) and (1b) require an initial condition and two boundary conditions for solution. The first (internal) boundary condition prescribes the temperature or heat flux density deep into the substrate. For the flat surfaces and road facet the appropriate condition is that the heat flux density G_{in} is zero at a distance sufficiently far into the surface to be inactive over the time-scale of the experiments. For the two wall facets and the roof facet the appropriate condition is that the interior (building) temperature T_{in} is prescribed. This form of the boundary condition does produce an anthropogenic heat source to the energy balance; in the results shown here this heat source is never larger than 4 W m^{-2}. The second boundary condition arises from the facet surface energy balances as described in the next subsection.

Equations (1a) and (1b) are solved by discretizing in the n-direction with the fluxes and temperatures staggered in the n-direction. The discretization used here has an outer layer which is 5 mm thick. This is sufficiently thin that the layer-averaged temperature for this layer, T_1, can be used in place of the skin temperature T_{sk} in those terms in the energy balance (Eq. (2)) for which this is needed, namely the emitted long-wave and sensible-heat flux densities (Smirnova *et al.* 1997).

(*b*) *Energy balance of the roughness sublayer*

The roughness sublayer acts to couple the substrate and the boundary layer. The total flux of momentum, i.e. the sum of the shear and dispersive stresses (Rotach 1999) is assumed constant with height across the roughness sublayer and hence equal to the value at z_* as determined by the roughness of the surface and the geostrophic forcing. We also assume that the mass of air within the roughness sublayer plays no role in the energetics of the volume. The flux of energy into the volume fabric is then equal to the flux density of energy into the building fabric integrated over the urban surface. Furthermore, the sensible-heat flux into the boundary layer, H_*, is determined as the composite of those from each facet.

Conservation of energy on each facet of the surface is governed by an energy balance, namely

$$(1-\alpha)S + L^{\downarrow} - L^{\uparrow} - H - G|_{n=0} = 0. \tag{2}$$

The facet-averaged flux densities S, $L^{\downarrow}$, $L^{\uparrow}$ and H denote the total incident solar, total incident long-wave and total outgoing long-wave radiation and sensible heat, respectively; α is the wavelength-averaged albedo of the surface. Standard solar geometry schemes are used to determine the facet-averaged direct solar fluxes (e.g. Owczarek 1997). The impact of geometry on the long-wave and diffuse solar fluxes, including multiple reflections, is accounted for using the matrix method for grey-body radiative transfer (e.g. Harman *et al.* 2004a). Equation (2) can be rearranged to provide the second boundary condition for Eq. (1) providing each of the terms in Eq. (2) can be expressed in terms of known variables. Note that we have assumed that urban areas are dry, and therefore the latent-heat term has been set to zero, to focus on the processes associated with a street canyon.

The long-wave radiation terms can be expressed, using Stefan's equation, as

$$L^{\downarrow} - L^{\uparrow} = L^{\downarrow} - \{\varepsilon\sigma T_1^4 + (1-\varepsilon)L^{\downarrow}\} = \varepsilon(L^{\downarrow} - \sigma T_1^4), \tag{3}$$

where ε is the wavelength-averaged emissivity of the surface, and the Stefan–Boltzmann constant $\sigma = 5.67 \times 10^{-8}$ W m^{-2}K^{-4}.

The sensible-heat flux density H is formulated using the bulk aerodynamic approach (e.g. Garratt 1992), namely

$$H = \rho c_p w_t (T_1 - \overline{\theta}(z_*)), \tag{4}$$

where ρ is density of air, c_p is the heat capacity of air at constant pressure, $\overline{\theta}(z_*)$ is the potential temperature at the reference level in the inertial sub-layer (see Fig. 1), and w_t is a transfer velocity dependent on the wind speed at the reference level. For the flat surface experiments the transfer velocity is expressed using the standard forms involving the roughness lengths for momentum and heat (e.g. Garratt 1992, pp. 40–84) with stability functions given by Beljaars and Holtslag (1991).

For the canyon surfaces, the transfer velocities are formulated through the resistance network model of Harman *et al.* (2004b), one of the innovations of the present formulation. This model recognizes that the bulk effects of the buildings, the local flow characteristics and the material roughness can all influence the flux of scalars from the urban surface. The model performs well against the observed transfer velocities representative of scalar flux densities from the facets of an urban street canyon (Barlow *et al.* 2004). In general, the transfer velocities from the facets of the urban street canyon are smaller than those of a flat surface of the same material under the same geostrophic forcing. The impact of atmospheric stability on the turbulent transport in urban areas is included by scaling each of the resistances in the above model by the same amount the resistance from a flat surface of equivalent effective roughness would experience in the same background stability. This approximation is not expected to influence results greatly as the influence of stability is reduced over high-roughness surfaces. However, note that this scaling does not account for small-scale buoyancy-driven flows which may influence the turbulent transfer close to the surface.

Studies have shown that a key aspect of the urban energy balance is that the energy balances of different building facets interact (Nunez and Oke 1977; Mills and Arnfield 1993). Here the energy balances of the four canyon facets interact in three ways. Firstly, the evolution of the boundary layer, and hence the reference level properties, depends on the cumulative effects of all four energy balances. Secondly, surface geometry impacts on the radiation terms of the canyon facets, i.e. S and $L^{\downarrow}$ for the urban canyon facets are geometry dependent and interact. Finally, the resistance network model for the sensible-heat flux allows for direct interaction between the fluxes from the canyon facets.

(*c*) *Momentum and energy balance of the boundary-layer evolution*

To allow for the natural coupling between the surface energy balance and boundary layer, the energy balance models have been coupled to the boundary-layer model of Busch *et al.* (1976). This is a one-dimensional, first-order closure, mixing-length-based model for the mean dynamic and thermodynamic profiles in the boundary layer. The equations for the horizontally homogeneous mean wind in the x- and y-directions ($\overline{u}$ and $\overline{v}$, respectively) and mean potential temperature $\overline{\theta}$ are

$$\frac{\mathrm{d}\overline{u}}{\mathrm{d}t} = -f(\overline{v} - v_g) - \frac{\mathrm{d}\overline{u'w'}}{\mathrm{d}z} = +f(\overline{v} - v_g) - \frac{\mathrm{d}}{\mathrm{d}z}\left(K_m \frac{\mathrm{d}\overline{u}}{\mathrm{d}z}\right), \tag{5a}$$

$$\frac{\mathrm{d}\overline{v}}{\mathrm{d}t} = -f(\overline{u} - u_g) - \frac{\mathrm{d}\overline{v'w'}}{\mathrm{d}z} = -f(\overline{u} - u_g) - \frac{\mathrm{d}}{\mathrm{d}z}\left(K_m \frac{\mathrm{d}\overline{v}}{\mathrm{d}z}\right), \tag{5b}$$

$$\frac{\mathrm{d}\overline{\theta}}{\mathrm{d}t} = -\frac{1}{\rho c_p}\frac{\mathrm{d}\overline{w'\theta'}}{\mathrm{d}z} - \frac{1}{\rho c_p}\frac{\mathrm{d}L_n}{\mathrm{d}z} = -\frac{1}{\rho c_p}\frac{\mathrm{d}}{\mathrm{d}z}\left(K_h \frac{\mathrm{d}\overline{\theta}}{\mathrm{d}z}\right) - \frac{1}{\rho c_p}\frac{\mathrm{d}L_n}{\mathrm{d}z}, \tag{5c}$$

where the overline indicates the time-mean and the primes are instantaneous deviations from that mean; u_g and v_g are the x- and y-components of the geostrophic wind, K_m and K_h are turbulent diffusivities for momentum and heat, respectively, formulated using the mixing-length analogy, and L_n is the net long-wave radiative flux density. The model requires a prescribed geostrophic pressure gradient and upper boundary conditions, taken as $\overline{u} = u_g$, $\overline{v} = v_g$ and $\overline{\theta}$ fixed. Lower boundary conditions for the thermodynamics are provided by H_* from the surface energy balance model and, for the dynamics, calculated from the (effective) roughness length for momentum and the reference level wind.

A simple two-stream radiative-transfer model (Edwards and Slingo 1996) is also included within the boundary-layer model, namely

$$L_n = L^+ - L^-, \tag{6a}$$

$$\frac{dL^\pm}{dz} = \pm\frac{5}{3}\frac{d\tau_a}{dz}\{L^\pm - \pi\sigma T^4 - \gamma(L^\mp - L^\pm)\}, \tag{6b}$$

where L^+ is the upwelling radiative flux density (positive upwards), L^- is the downwelling radiative flux density (positive downwards), τ_a is the absorptive optical depth, γ is a coefficient accounting for the effects of scattering, and the $5/3$ term arises from hemispheric integration. These equations are primarily used to provide a consistent formulation for the flux density of downwelling long-wave radiation to the surface, $L^-(z = z_*)$. Estimates of the cooling in the boundary layer due to radiative flux divergence are also calculated (the L_n term in Eq. (5c)). Constant values for the radiative-transfer properties ($d\tau_a/dz$ and γ) are assumed throughout the boundary layer; this is unlikely to be true in reality but is unlikely to impact on the principal results shown.

(*d*) *Initial conditions*

The above subsections describe a self-contained model for the evolution of the boundary layer, surface energy balance and substrate over dry homogeneous terrain. A number of external parameters are needed to formulate the terms within the model. These are the location and times for the experiments, the material albedo and emissivity, the volumetric heat capacity and thermal conductivity, the roughness length for momentum for the surface material, the geostrophic pressure gradient, and initial conditions on the thermodynamic component of the model. The roughness length for heat of the surface material and individual facets is assumed to be one tenth of that for momentum (e.g. Garratt 1992)†.

Figure 2 shows the initial conditions for the thermodynamic component of the model. The models are initialized at dusk. The initial temperature profiles within the substrate (Fig. 2(a)) are calculated by passing a surface temperature wave of amplitude 10 K into the substrate (Eq. (1)) subject to the appropriate boundary conditions.

The initial atmospheric potential-temperature profile used (Fig. 2(b)) is comprised of three layers. From the bottom upwards, these are a well-mixed layer extending up to a highly stable layer, which forms a capping inversion, and finally a stable (non-turbulent) layer in the free troposphere. In the results shown the atmosphere above 1 km remains essentially unchanged through the integrations.

† In this problem there are two values each of the thermal and momentum roughness lengths. Firstly, those of the materials of the facets, and secondly, those 'effective' values of the whole urban surface. It is the effective values that are typically measured (e.g. by Voogt and Grimmond 2000). In the model we need to specify the material values. The effective values are computed as part of the model, through the turbulent transfer model of Harman *et al.* (2004b), and depend upon canyon geometry, time of day etc. The calculated effective values are several orders of magnitude smaller than 0.1 and closer to observations.

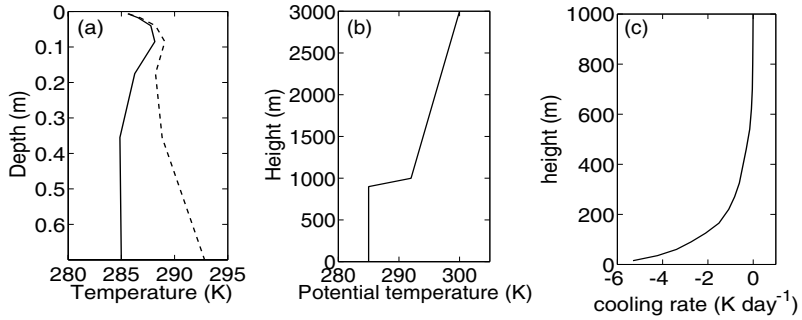

Figure 2. Initial conditions used for the thermodynamic component of the model. (a) Temperature profile in the substrate, flat surfaces and street facet (solid line), wall and roof facets (dashed). (b) Potential-temperature profile. (c) Cooling rate due to long-wave radiative flux divergence.

Radiative-transfer processes in the atmosphere usually result in cooling of the boundary layer through flux divergence. Figure 2(c) shows a calculation of the radiative cooling rate based on the initial potential-temperature profile. Cooling is concentrated in the lowest layers of the boundary layer with the upper profile (not shown) taking small (positive) values. The inclusion of this term does not significantly change the results shown here except that it helps to prevent divergence of the model states during the integration. Results will be shown from the second model day to allow for initial adjustments but to minimize the drift between different model runs.

A first estimate for the dynamic initial conditions are given by

$$u(z) = \begin{cases} u_{\mathrm{g}} \ln\left(\dfrac{z-d}{z_{T\mathrm{m}}}\right) \Big/ \ln\left(\dfrac{h-d}{z_{T\mathrm{m}}}\right), & \text{for } 0 < z < h, \\ u_{\mathrm{g}}, & \text{for } z \geq h, \end{cases} \tag{7}$$

where $z_{T\mathrm{m}}$ is the effective roughness length for momentum (for flat surfaces this is equal to the material roughness length), d is the displacement height of the surface and $h = 1$ km is the initial height of the boundary layer. For the urban experiments, the effective roughness length and displacement height are calculated from the surface morphology using the model of MacDonald *et al.* (1998).

4. Results from the coupled energy balance–boundary layer system

The characteristics of urban climate identified in section 2 are now investigated by analysing results from four configurations of the model. We consider synoptic conditions where we expect large impacts of the urban area, namely clear skies and light winds (Oke 1987). Consequently, we take a geostrophic pressure gradient that gives a dynamic forcing of $u_{\mathrm{g}} = 5$ m s^{-1} and $v_{\mathrm{g}} = 0$ m s^{-1}. The surfaces are located at 60°N with surface material properties, unless stated otherwise, of $\alpha = 0.3$, $\varepsilon = 0.98$, $k = 0.75$ W m^{-1}K^{-1}, $C_{\mathrm{s}} = 1.5 \times 10^6$ J K^{-1}m^{-3}, a material roughness length for momentum $z_{0\mathrm{m}} = 0.01$ m and that for heat $z_{0\mathrm{h}} = 0.1 z_{0\mathrm{m}}$†. These values of the material roughness lengths are typical of a range of surface materials used in urban areas (e.g. Oke 1987; Garratt 1992). The model is then configured as:

† See previous footnote.

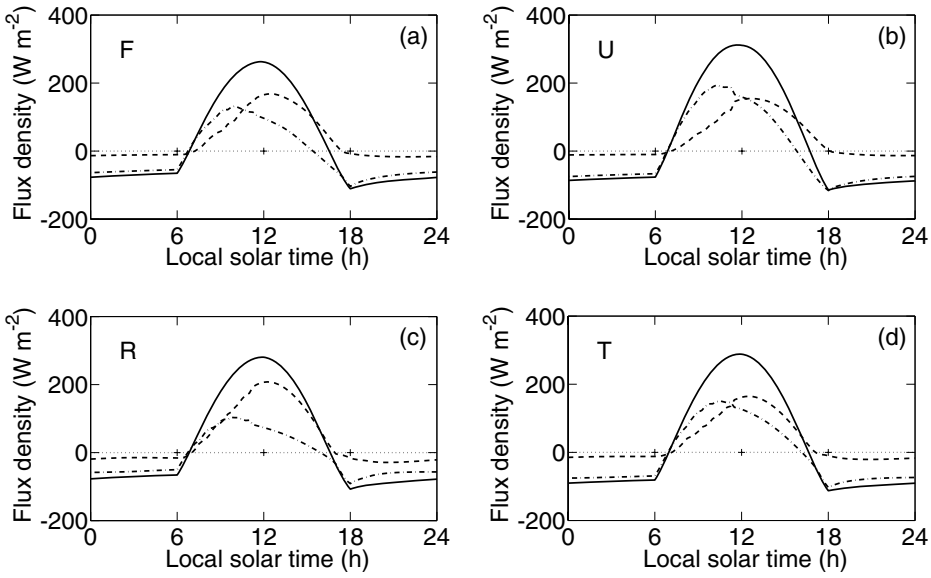

Figure 3. Diurnal energy balance profiles from the coupled models: net radiation flux density (solid line), sensible-heat flux density (dashed), and ground heat flux density (residual, dash-dotted). (a) Case $\mathcal{F}$, (b) case $\mathcal{U}$, (c) case $\mathcal{R}$ and (d) case $\mathcal{T}$ (see text).

(i) Case $\mathcal{F}$: a flat surface with surface material properties given above.

(ii) Case $\mathcal{U}$: an urban street canyon with $h_e = 10$ m, $h_e/w_e = 1.0$ and $w_e/r_e = 0.5$ (see Fig. 1), representative of a built-up part of a city. The urban street canyon is oriented north–south. The properties of the surface material are as in case $\mathcal{F}$. The building morphology leads to an effective roughness length for momentum of $z_{T\mathrm{m}} = 0.53$ m.

(iii) Case $\mathcal{R}$: a flat surface where the material roughness length takes the same value as that of the urban street canyon unit, namely $z_{0\mathrm{m}} = 0.53$ m, and the roughness length for temperature is taken to be $z_{0\mathrm{h}} = 0.1 z_{0\mathrm{m}}$.

(iv) Case $\mathcal{T}$: a flat surface with the same roughness lengths as case $\mathcal{R}$, but with the surface thermal properties altered to have the same effective values as those of the urban street canyon, namely $C_s = 3.0 \times 10^6$ J K^{-1}m^{-3}, $k = 1.5$ W m^{-1}K^{-1}.

Figure 3 illustrates results from these simulations over a diurnal cycle. We consider the daytime and night-time balances separately.

(*a*) *Daytime energy balance*

We begin by considering the daytime budgets. During the morning the net radiation increases with the increasing direct solar forcing. At early times, the urban surface is cooler than the overlying boundary layer because of cooling the night before. Hence during a *morning transition* period the positive net radiation is taken up by the ground heat flux, which warms the substrate and the surface temperature. When the surface temperature exceeds the boundary-layer temperature, convection is initiated with a positive sensible-heat flux from the surface into the boundary layer, which erodes the nocturnal stably stratified boundary layer. All four cases follow this evolution, with the ground heat flux peaking in the morning and the sensible heat peaking in the afternoon.

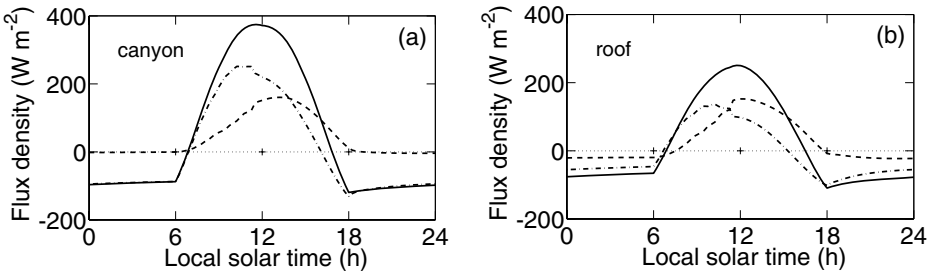

Figure 4. Diurnal energy balance profiles for (a) the canyon fraction and (b) the roof fraction of case $\mathcal{U}$. Lines as in Fig. 3.

All the terms of the energy balance are different between the urban case $\mathcal{U}$ and the flat case $\mathcal{F}$. During the day the magnitude of the net radiation is increased slightly, the ground heat is increased and the sensible-heat flux is slightly decreased compared to case $\mathcal{F}$. The phasing of the terms are also changed, with the peak value of the ground heat flux half an hour earlier and the peak in the sensible-heat flux one hour later. The net radiation peaks at about midday in both cases. These changes are in agreement with the observed characteristics of urban areas when compared with rural surroundings that were identified in section 2 (Cleugh and Oke 1986; Grimmond *et al.* 1993).

The physical processes responsible for these changes can be understood by considering the results from cases $\mathcal{R}$ and $\mathcal{T}$. When compared to case $\mathcal{F}$, increasing the roughness of a flat surface (case $\mathcal{R}$) increases the efficiency of turbulent transfer from the surface. This increases the magnitude of the sensible-heat flux and causes the peak value to occur earlier. These changes are in the opposite sense to the differences between cases $\mathcal{F}$ and $\mathcal{U}$. Yet urban areas are undeniably aerodynamically rougher than a planar surface. Results (not shown) for a flat surface with thermal properties taken to be equal to the effective values of the urban surface, but with a small roughness, tend to shift the energy balance in the opposite direction. Case $\mathcal{T}$, which has the same effective thermal properties as the urban surface and the higher roughness length, leads to a ground heat flux of the correct phase, but with smaller magnitude, and with the peak sensible-heat flux occurring too early because of the enhanced mixing by the higher surface roughness. Clearly effects of building form, which are not accounted for in cases $\mathcal{R}$ or $\mathcal{T}$, play a critical role in the urban energy balance.

The street canyon model, case $\mathcal{U}$, has extra freedom compared to the flat surface, because it consists of separate energy balances for four active surfaces, namely the roof, street and two walls. The surface temperatures of these elements then evolve differently. To illustrate this aspect of the model, Fig. 4 shows separately the energy balance of the street canyon (combined street and two walls) and roof. The urban energy balance of case $\mathcal{U}$ is the area-weighted sum of these two balances. A striking aspect of Fig. 4 is the large ground heat flux into the canyon fraction during the morning. This explains the increase in the ground heat flux density between case $\mathcal{T}$ and case $\mathcal{U}$, and is itself caused by three processes. Firstly, the canyon fraction has a higher surface area than a flat surface and so requires more energy to raise the surface temperature to above the boundary-layer temperature. Hence the early morning transition, where the net radiation is almost entirely balanced by the ground heat flux, persists longer into the morning than for a flat surface. Secondly, the amount of downwelling solar radiation absorbed in the street canyon is higher than the flat surface, because some of the radiation reflected from one facet is incident upon another facet where a further fraction is absorbed,

before it is reflected again. Finally, the transfer velocities w_t that mediate sensible-heat flux for the canyon facets are reduced by geometric effects on the canyon flow (Harman *et al.* 2004b). In this way, more energy is absorbed into the fabric of an urban surface, extending the morning transition and delaying the onset of convective heat flux into, and so also warming of, the boundary layer. This analysis suggests a sensitivity of the urban energy balance to the fraction of coverage of roof compared to street.

(*b*) *Night-time energy balance*

Just after sunset each of the cases in Fig. 3 shows an *evening transition*, when the surface temperature cools until it is below the boundary-layer air temperature. A heat flux from the boundary layer then cools air in the lower layers and generates a stably stratified boundary layer. The effects of surface area and the limited sky view are again prominent in the urban energy balance. Increased surface area yields an increased total emission of long-wave radiation. A significant fraction of this radiation is incident upon, and absorbed by, other canyon facets, and so does not escape to space. The magnitude of the net flux density of radiation at the canyon facets is reduced and so they cool more slowly than a flat surface. The canyon surface temperatures therefore remain higher, yielding in turn a greater emittance of long-wave radiation. This then gives the increased magnitude of the net radiation from the canyon fraction of case $\mathcal{U}$.

A further feature of the nocturnal energy balance which is apparent in Fig. 4 is that almost all the nocturnal sensible-heat flux originates from the roof. The canyon fraction in this case has almost zero sensible-heat flux. The loss of heat from radiative cooling in the street canyon is balanced almost entirely by the conduction of heat stored in the building fabric. The roof surface, in the model at least, behaves like a flat surface, with a small sensible-heat flux from the boundary layer into the roof, cooling the boundary layer. Overall, the sensible-heat flux from the urban case $\mathcal{U}$ is slightly negative, and the boundary layer cools only slowly. Thus, the evening transition is extended over the urban surface, which delays transition to stable conditions by approximately two hours compared to the other cases. However, the observed characteristic that the sensible-heat flux can remain positive throughout the night (e.g. Grimmond and Oke 2002; Christen and Vogt 2004) is not found in this simulation. This issue is taken up again in section 6.

(*c*) *Temperature profiles in the boundary layer*

Differences in the surface energy balances are reflected in the differences between the accompanying boundary-layer potential-temperature profiles as shown in Fig. 5. Although the energy balances for the different cases showed the largest differences by day, the daytime boundary-layer potential-temperature profiles are quite similar. The reason is that in the simulations the daytime boundary layer is deep (of order 1 km), so that the differences in surface forcing are spread over a greater depth, and are therefore smaller. (Clearly differences during daytime would be greater if the boundary layer were constrained to be shallower by large-scale meteorological processes.) Conversely, even the small differences in the night-time energy balances yield large differences in the temperature profiles of the shallow nocturnal boundary layer.

Cases $\mathcal{F}$ and $\mathcal{R}$ show a stable temperature profile after sunset (1800 local solar time). As shown in Fig. 3, through the night the sensible-heat flux is small and the dominant balance in the energy balance is between the ground heat flux and radiation, which therefore control the surface temperature. Since cases $\mathcal{F}$ and $\mathcal{R}$ have the same thermal and radiative properties, the surface temperatures are similar.

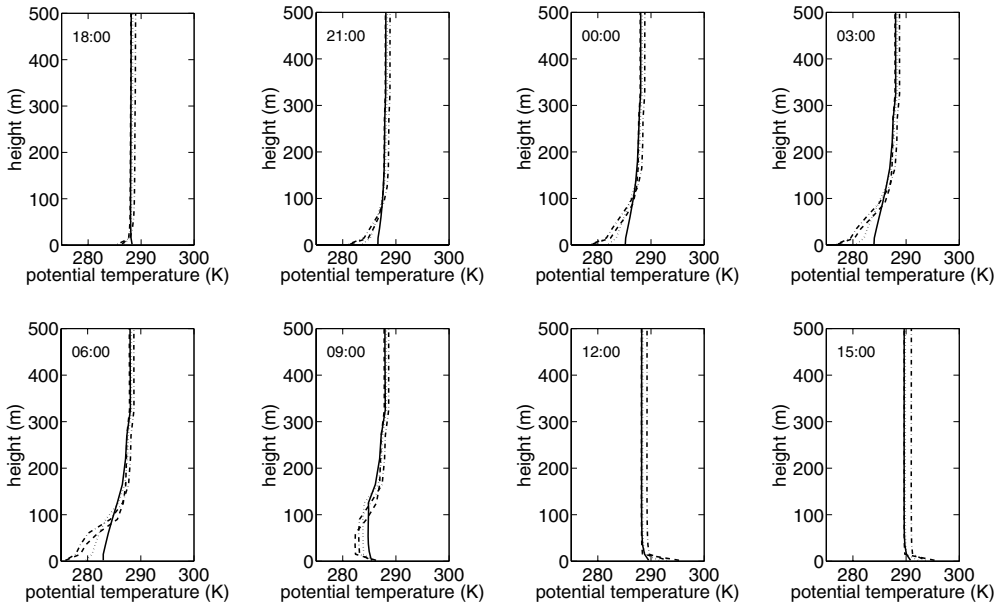

Figure 5. Potential-temperature profiles for the lowest 500 m of the atmosphere: case $\mathcal{U}$ (solid line), case $\mathcal{F}$ (dashed), case $\mathcal{R}$ (dash-dotted) and case $\mathcal{T}$ (dotted line). Local solar time is marked on each plot.

As argued previously, case $\mathcal{U}$ has a reduced surface cooling rate because of the combined geometric impacts on the emission of radiation to space. Hence the urban case $\mathcal{U}$ shows a weaker stable stratification through the night. The temperature difference between cases $\mathcal{U}$ and $\mathcal{F}$ grows through the night. Observations suggest a maximum urban to rural temperature contrast occurs near midnight and then reduces through the remainder of the night (e.g. Oke 1987). Surface moisture, not represented here, plays an important role in the rural energy balance and may be responsible for this difference. Case $\mathcal{T}$, with its intermediate energy balance, has potential-temperature profiles which fall in between those of case $\mathcal{U}$ and cases $\mathcal{F}$ and $\mathcal{R}$, though differences in timings do occur.

The depth of the nocturnal boundary layer over the urban surface, determined as the lowest height where the gradient Richardson number exceeds $1/4$, is more than twice that in cases $\mathcal{F}$ and $\mathcal{R}$ and one and a half times that of case $\mathcal{T}$. The mechanisms responsible illustrate how the energy balance and boundary-layer processes work together. The reduced rate of surface cooling over the urban surface leads to a less pronounced stable stratification through the boundary layer, which inhibits less the turbulent mixing through the stable boundary layer. This allows heat to be mixed down from higher levels in the residual daytime boundary layer to the surface, which helps resist further the formation of a stronger stable stratification in the boundary layer.

These model runs show that the main characteristics of the urban energy balance–boundary layer system can be captured. An important aspect of the model is that the energy balances of the roof and street canyon surfaces are treated separately. This allows the magnitudes and phasing of the terms in the energy balance to vary (as in observations of the urban energy balance, e.g. Grimmond and Oke (2002)) in a way which cannot be achieved with the single-surface model.

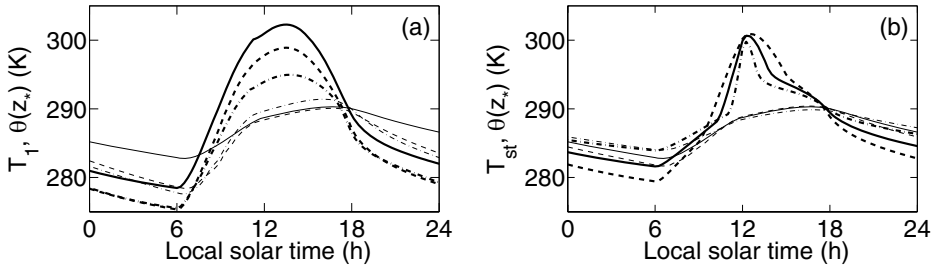

Figure 6. Diurnal variation of the surface temperatures (thick lines) and reference-level air temperature (thin lines) for different model configurations. (a) Roof surface and reference-level temperatures from case $\mathcal{U}$ (solid lines), with $h_e/w_e = 1.0$, $w_e/r_e = 0.5$, $h_e = 10$ m (see Fig. 1), case $\mathcal{F}$ (dashed) and case $\mathcal{R}$ (dash-dotted). Case $\mathcal{T}$ not included for clarity. (b) Street surface and reference-level temperatures from case $\mathcal{U}$, with $w_e/r_e = 0.5$, $h_e = 10$ m: $h_e/w_e = 0.5$ (solid lines), $h_e/w_e = 1.0$ (dashed) and $h_e/w_e = 2.0$ (dash-dotted).

5. SURFACE TEMPERATURES AND BOUNDARY-LAYER TEMPERATURES

The aim of this section is to establish how building form controls the temperatures of the urban surfaces and air temperatures at the lowest level, $z = z_*$, in the boundary layer. Figure 6 shows the diurnal variation of surface temperatures from cases $\mathcal{F}$ and $\mathcal{R}$ together with the street surface temperature from case $\mathcal{U}$ for a range of canyon geometries. For the flat surface, cases $\mathcal{F}$ and $\mathcal{R}$ (Fig. 6(a)), increasing the roughness increases the sensible-heat flux and more tightly couples the surface to the boundary-layer temperatures. The maximum daytime surface temperature is therefore reduced and the boundary-layer temperature increased. The surface temperature of the roof of the urban surface from case $\mathcal{U}$ (Fig. 6(a)) follows a similar pattern, but with a higher daytime maximum temperature, because the roof surface is represented here as having a low roughness. Pitched roofs might be represented by a higher roughness, which would bring the daytime profiles closer together. At night the boundary layer over the flat surface becomes stably stratified, and little heat transfer is possible from the boundary layer into the surface, and so the surface temperature drops rapidly. The roof of the urban surface remains warmer than the flat surface $\mathcal{F}$ because the urban boundary layer remains more nearly neutrally stratified, enabling more turbulent heat transfer.

The temperatures of the street canyon facets warm strongly only during the limited times when incoming solar radiation is directly incident. At other times shadowing reduces the incoming radiation. Figure 6(b) shows this process for the street facet. The period of hottest daytime street temperatures reduces as the canyon aspect ratio, h_e/w_e, is increased (but with the fraction of roof kept constant). At night the limited sky view exerts a geometric constraint on outgoing long-wave radiation. The street surface then remains about 5 K warmer than the flat surface. Figure 6(b) also shows that as the canyon aspect ratio, h_e/w_e, is increased (but with a constant roof fraction) so the cooling of the road surface is progressively arrested, as found by Oke *et al.* (1991) in a simpler modelling study. In this sense the local building form strongly controls surface temperature in urban areas.

Figure 6 also shows the evolution of the air temperature at the lowest level in the boundary layer. Over the flat surface the diurnal range of boundary-layer temperatures is smaller than the range of surface temperatures. The boundary-layer temperature is heated by the sensible-heat flux from the surface by day and cooled by sensible-heat flux to the surface by night. Hence the boundary layer is always following the surface temperature. During the day the temperature of the lowest level of the boundary layer is similar for all simulations shown. There are two main reasons.

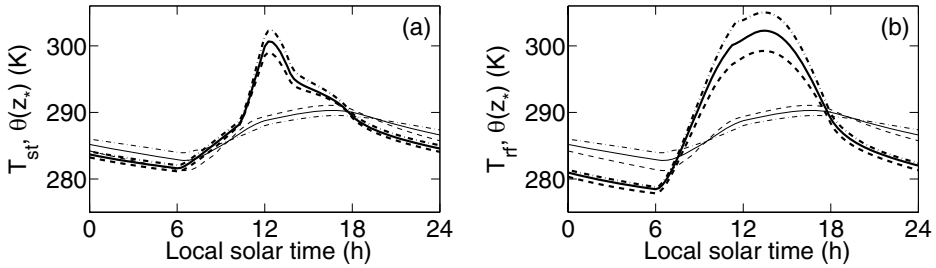

Figure 7. Diurnal variation of the surface temperatures (thick lines) and reference-level air temperature (thin lines) for different configurations of case $\mathcal{U}$ with $h_e/w_e = 1.0$, $h_e = 10$ m. (a) Street surface and reference-level temperatures, and (b) roof surface and reference-level temperatures: $w_e/r_e = 0.3$ (dashed), $w_e/r_e = 0.5$ (solid lines) and $w_e/r_e = 0.7$ (dash-dotted).

Firstly, as mentioned above, the depth and uniformity in temperature of the daytime boundary layer means large heat changes can be accommodated by small temperature changes and by deepening of the boundary layer. Secondly, the heat flux from the urban surface is not strongly sensitive to h_e/w_e when w_e/r_e is kept fixed. The tendency for the heat flux from the street canyon to increase because surface area increases with increasing h_e/w_e is largely offset by the reduction in heat flux from the street canyon because the local flow adjacent to the surface is reduced as h_e/w_e increases. By night the local boundary-layer temperature over the urban surface is much higher than over the flat surface because the surface cooling is reduced by the limited sky view, which reduces as h_e/w_e increases, as explained earlier.

Figure 7 shows the variation of surface and boundary-layer temperatures with a second measure of building form, w_e/r_e, which measures the fraction of surface occupied by street canyon rather than roof surface. As this parameter is varied so h_e/w_e is kept constant. Figure 7(a) then confirms that the night-time temperature of the street, which is controlled by the nocturnal radiation budget, which is determined largely by h_e/w_e, also remains largely the same. Similarly, the night-time roof temperature (Fig. 7(b)) varies little with w_e/r_e as this parameter does not directly affect the roof surface radiation budget. Figure 7 also shows the effect of w_e/r_e on the temperature of the lowest level in the boundary layer. As w_e/r_e decreases, so the fraction of roof surface increases and the diurnal cycle of $\overline{\theta}(z_*)$ becomes larger. In the limit of all roof surface, $\overline{\theta}(z_*)$ follows the diurnal cycle of a displaced flat surface of low roughness. The addition of the canyon fraction moderates this diurnal cycle, by changing the heat flux into the boundary layer as previously described. Comparing Figs. 6 and 7, we conclude that the boundary-layer air temperatures are controlled more by the fraction of roof surface rather than the canyon aspect ratio, h_e/w_e.

6. NOCTURNAL HEAT FLUX

During the night the boundary layer typically becomes stably stratified, reducing the turbulent mixing. Such stable conditions pose problems for observations because of, for instance, intermittency in the turbulent mixing and the large source areas of measurements. However a common, and important, characteristic of urban climates is the tendency for positive sensible-heat fluxes, and neutral boundary layers at night (Grimmond and Oke 2002). Anthropogenic heating is one possible mechanism to explain this feature but is it the only physically plausible mechanism? Here we explore two further mechanisms that also serve to demonstrate further sensitivities of the model.

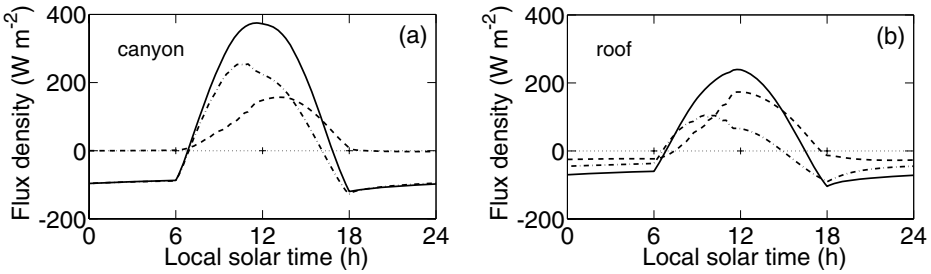

Figure 8. Diurnal energy balance profiles for (a) the canyon fraction and (b) the roof fraction of case $\mathcal{U}$ with modified material properties as described in the text. Lines as in Fig. 3.

(*a*) *Heterogeneity from roof and street canyon*

A first possible alternative mechanism is demonstrated by running the model with different material properties for the roof and street canyon facets: the heat capacity of the roof material is $C_s = 0.75 \times 10^6$ J K^{-1}m^{-3}, half the value used in case $\mathcal{U}$. All other parameters take the same values. Figure 8 shows the evolution of the energy balance for the canyon and roof fractions. The low thermal mass of the roof surface reduces the ground heat flux into the roof. Both the sensible-heat and long-wave-radiation fluxes change to compensate. In particular, by night there is greater sensible-heat flux from the boundary layer to the roof. This cools the boundary-layer air so much that it is cooler than the surface temperatures in the street canyon, which as before remain warmer through the combination of high heat capacity and reduced sky view. The result is a (small) positive sensible-heat flux from the street canyon into the boundary layer throughout the night. A measurement technique that is biased towards the canyon fraction of the surface would then indicate a positive flux when the total flux is still negative. Such potential issues with instrument location (e.g. the mismatch of radiometer and anemometer source areas) and observation analysis have been identified in recent observation campaigns (Grimmond *et al.* 2004; Christen and Vogt 2004).

(*b*) *Role of advection*

The sensible-heat flux into the boundary layer depends on the difference between the air temperature and the surface temperature. If the boundary-layer air evolves independently of the local surface energy balance, then the air can remain cooler than the surface, yielding a positive nocturnal heat flux. The boundary layer is so decoupled from the local surface energy balance when advection carries air adjusted to one surface over a new surface, for example advection from a rural to urban surface.

A full simulation of advection is beyond the scope of this paper. But a first assessment of this mechanism can be made by running the surface energy balance model for case $\mathcal{U}$ forced by boundary-layer properties obtained from the coupled system in case $\mathcal{F}$. The surface-only model requires the flux of downwelling long-wave radiation, winds and potential temperature at the reference level z_*. Figure 9 shows the energy balance of the urban surface (Fig. 9(a), which should be compared with Fig. 3), and of the street canyon fraction (Fig. 9(b), which should be compared with Fig. 4) forced in the uncoupled way.

During the day the magnitude of the fluxes from the uncoupled case are similar to the coupled case. However, the phasing of the fluxes is different: the ground heat flux is delayed and the sensible-heat flux is advanced, and are similar to the results

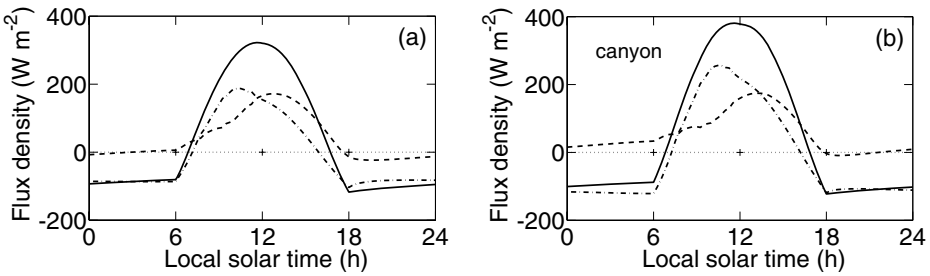

Figure 9. Diurnal energy balance profiles for (a) the total and (b) the canyon fraction of case $\mathcal{U}$, when run in surface-only mode with forcing from case $\mathcal{F}$. Lines as in Fig. 3.

from case $\mathcal{F}$. During the night, there are qualitative differences. A positive sensible-heat flux is maintained after sunset, then drops to being slightly negative and then increases through the night, becoming positive again before sunrise. The reason is that the boundary-layer air temperature evolves separately from the surface temperature. Although the details of the behaviour seen here are different to observations (e.g. Grimmond and Oke 2002), the simulation serves to show how local advection might lead to positive nocturnal heat fluxes.

7. Conclusions

Urban areas have distinct climates that have several generic features (described in section 2). There is a bewildering array of different possible effects of urban areas on the atmosphere and so the aim of this paper has been to identify the dominant physical processes responsible for this distinct climate. We have addressed this aim by developing a reasonably complete model for the energy balance of a simple street geometry. Novel aspects of the model are in the parametrization of the sensible-heat flux, which has been validated against wind tunnel observations (Harman *et al.* 2004b), and the radiation calculation, which accounts for multiple reflections and shadowing (Harman *et al.* 2004a). Following the motivation to understand a relatively simple model, we have assumed that the latent-heat flux and the anthropogenic heat flux are both zero. This energy balance model has then been coupled to a model for the atmospheric boundary layer. The coupled model has been run and the results analysed to establish the dominant physical mechanisms that lead to generic features of urban climate. While recognizing the idealized nature of this study, we now relate the main findings of the study to the observed generic characteristics of the urban climate, summarized in section 2, and offer suggestions for how these findings might generalize to more complex urban geometries, and how the parameters of the model might be configured to compare with observations.

Firstly, we have seen how the energy balance, and in particular the sensible-heat flux, for the roof surface is very different from the energy balance of the street canyon. This means that the sensible-heat flux into the boundary layer, the weighted average of the roof and street-canyon heat fluxes, depends strongly on the plan area index λ_p, the fraction of surface (looking down from vertical) covered by roof compared to street. In this way we expect λ_p to be an important parameter in determining the low-level air temperatures in urban areas. The heterogeneity between fluxes from the roof and street canyon may well contribute to the heterogeneity observed by Schmid *et al.* (1991).

Secondly, we have seen how the evening and morning transition periods, around sunrise and sunset, are characterized by the ground heat flux balancing net radiation.

The prolonged morning transition seen in the model is consistent with the observation that the ground heat flux/storage term is larger than the sensible-heat flux over much of the day. It is often said that it is the large heat capacity of construction materials used in urban areas that is important. But the simulations have shown that the important physical variable is the heat capacity of the active volume of building material, which is the product of surface area in contact with the air, the depth of penetration of the heat (which depends on the heat conductivity) and specific heat capacity of the material. Since this quantity is larger in urban areas, they need to absorb large amounts of heat to change their surface temperature, and so the morning and evening transitions persist longer than in rural areas. This analysis explains why the ground heat/storage term often peaks earlier and the sensible-heat flux later than for rural areas.

Thirdly, we have seen how there are substantial changes to the radiation budget in urban areas. As suggested by several other authors, we have found that the local sky view largely controls the flux of outgoing long-wave radiation, and incoming long- and short-wave radiation. Since the net radiation is the driving flux for the temperatures of the surfaces, this explains Bärring's (1985) observation that surface temperatures are determined largely by local building form, which for the two-dimensional geometry studied here is parametrized as h_e/w_e.

Fourthly, we have seen that the sensible-heat flux from the surface is controlled by the surface area and by the efficiency of the local flow to move heat away from the surface, parametrized here as a transfer velocity. For the two-dimensional street considered here these two effects largely cancel one another: as h_e/w_e increases so the surface area increases, but at the same time the local flow speeds within the street reduce. This finding from the model helps explain Bärring's (1985) observation that air temperature does not correlate as well as street surface temperature with local building form. An important remaining question is whether or not this cancellation follows for more complex three-dimensional geometries.

Fifthly, under ideal conditions the daytime convective boundary layer evolves similarly over the flat and urban surfaces, despite the daytime surface fluxes being different. The reason is that daytime convective boundary layer is deep and can accommodate moderate changes in heat content with only small changes in temperature. This suggests that there may well be larger differences between the rural and urban daytime boundary layers in conditions of large-scale descent, such as anticyclones.

Finally, we have considered two possible explanations of the observation that the sensible-heat flux in urban areas can remain positive through the night. The heterogeneity between the energy balance of the roof and street canyon can lead to the roof cooling the boundary-layer air faster than the street canyon surfaces cool, leading to positive sensible-heat flux from the street canyon. Larger-scale heterogeneity leads to systematic advection, so that the boundary-layer air is decoupled from the surface energy balance below. In this way cool boundary-layer air, perhaps from a neighbouring rural area, can be advected over a warmer urban surface leading to a positive sensible-heat flux. Answering this question definitively will require skilled measurements and skilled interpretation.

ACKNOWLEDGEMENTS

This work forms part of the UWERN Urban Meteorology Programme (www.met.reading.ac.uk/Research/urb_met/), and was funded by the Natural Environment Research Council and the Met Office (NER/S/A/2000/03555). The first author gratefully acknowledges support from the DAPPLE project (www.dapple.org.uk) and

Commonwealth Scientific and Industrial Research Organisation Marine and Atmospheric Research (www.cmar.csiro.au). Thanks are also due to Martin Best and Janet Barlow for valuable discussions.

REFERENCES

Arnfield, A. J. 2003 Two decades of urban climate research: A review of turbulence, exchanges of energy and water, and the urban heat island. *Int. J. Climatol.*, **23,** 1–26

Arnfield, A. J. and Grimmond, C. S. B. 1998 An urban canyon energy budget model and its application to urban storage heat flux modeling. *Energ. Build.*, **27,** 61–68

Barlow, J. F. and Belcher, S. E. 2002 A wind tunnel model for quantifying fluxes in the urban boundary layer. *Boundary-Layer Meteorol.*, **104,** 131–150

Barlow, J. F., Harman, I. N. and Belcher, S. E 2004 Scalar fluxes from urban street canyons. Part I: Laboratory simulation. *Boundary-Layer Meteorol.*, **113,** 369–385

Bärring, L., Mattsson, J. O. and Lindqvist, S. 1985 Canyon geometry, street temperatures and the urban heat island in Malmö, Sweden. *J. Climatol.*, **5,** 433–444

Belcher, S. E., Jerram, N. and Hunt, J. C. R. 2003 Adjustment of a turbulent boundary layer to a canopy of roughness elements. *J. Fluid Mech.*, **488,** 369–398

Beljaars, A. C. M. and Holtslag, A. A. M. 1991 Flux parameterization over land surfaces for atmospheric models. *J. Appl. Meteorol.*, **30,** 327–341

Best, M. J. 2005 Representing urban areas within operational numerical weather prediction models. *Boundary-Layer Meteorol.*, **114,** 91–109

Busch, N. E., Chang, S. W. and Anthes, R. A. 1976 A multi-level model of the planetary boundary layer suitable for use with mesoscale dynamic models. *J. Appl. Meteorol.*, **15,** 909–919

Christen, A. and Vogt, R. 2004 Energy and radiation balance of a central European city. *Int. J. Climatol.*, **24,** 1395–1421

Cleugh, H. A. and Oke, T. R. 1986 Suburban–rural energy balance comparisons in summer for Vancouver, BC. *Boundary-Layer Meteorol.*, **36,** 351–369

Coceal, O. and Belcher, S. E. 2004 A canopy model of mean winds through urban areas. *Q. J. R. Meteorol. Soc.*, **130,** 1349–1372

Dabberdt, W. F., Hales, J., Zubrick, S., Crook, A., Krajewski, W., Doran, J. C., Mueller, C., King, C., Keener, R. N., Bornstein, R., Rodenhuis, D., Kocin, P., Rossetti, M. A., Sharrocks, F. and Stanley, E. M. 2000 Forecast issues in the urban zone: Report of the 10th Prospectus Development Team of the US Weather Research Program. *Bull. Am. Meteorol. Soc.*, **81,** 2047–2064

Dabberdt, W. F., Carroll, M. A., Baumgardner, D., Carmichael, G., Cohen, R., Dye, T., Ellis, J., Grell, G., Grimmond, S., Hanna, S., Irwin, J., Lamb, B., Madronich, S., McQueen, J., Meagher, J., Odman, T., Pleim, J., Schmid, H. P. and Westphal, D. L. 2004 Meteorological research needs for improved air quality forecasting—Report of the 11th prospectus development team of the US Weather Research Program. *Bull. Am. Meteorol. Soc.*, **85,** 563–586

Edwards, J. M. and Slingo, A. 1996 Studies with a flexible new radiation code. I: Choosing a configuration for a large-scale model. *Q. J. R. Meteorol. Soc.*, **122,** 689–719

Garratt, J. R. 1992 *The atmospheric boundary layer.* Cambridge University Press

Grimmond, C. S. B. and Oke, T. R. 1995 Comparison of heat fluxes from summertime observations of suburbs of four North American cities. *J. Appl. Meteorol.*, **34,** 873–889

1999 Heat storage in urban areas: Local-scale observations and evaluation of a simple model. *J. Appl. Meteorol.*, **38,** 922–940

2002 Turbulent heat fluxes in urban areas: Observations and a local-scale urban meteorological parameterization scheme (LUMPS). *J. Appl. Meteorol.*, **41,** 792–810

Grimmond, C. S. B., Oke, T. R. and Cleugh, H. A. 1993 The role of "rural" in comparisons of observed suburban–rural flux differences. *IAHS Publ.*, **212,** 165–174

Grimmond, C. S. B., Salmond, J. A., Oke, T. R., Offerle, B. and Lemonsu, A.	2004	Flux and turbulence measurements at a densely built-up site in Marseille: Heat, mass (water and carbon dioxide), and momentum. *J. Geophys. Res. Atmos.*, D24101
Hacker, J. N., Belcher, S. E. and Connell, R. K.	2005	Beating the heat: Keeping UK buildings cool in a warming climate. UKCIP Briefing Report. UKCIP, Oxford, UK
Harman, I. N., Best, M. J. and Belcher, S. E.	2004a	Radiative exchange in an urban street canyon. *Boundary-Layer Meteorol.*, **110,** 301–316
Harman, I. N., Barlow, J. F. and Belcher, S. E.	2004b	Scalar fluxes from urban street canyons. Part II: Model. *Boundary-Layer Meteorol.*, **113,** 387–409
Ichinose, T., Shimodozono, K. and Hanaki, K.	1999	Impact of anthropogenic heat on urban climate in Tokyo. *Atmos. Environ.*, **33,** 3897–3909
MacDonald, R. W., Griffiths, R. F. and Hall, D. J.	1998	An improved method for the estimation of surface roughness of obstacle arrays. *Atmos. Environ.*, **32,** 1857–1864
McNaughton, K. G. and Spriggs, T. W.	1986	A mixed-layer model for regional evaporation. *Boundary-Layer Meteorol.*, **34,** 243–262
Martilli, A., Clappier, A. and Rotach, M. W.	2002	An urban surface exchange parameterisation for mesoscale models. *Boundary-Layer Meteorol.*, **104,** 261–304
Mason, P. J.	1988	The formulation of areally averaged roughness lengths. *Q. J. R. Meteorol. Soc.*, **114,** 399–420
Masson, V.	2000	A physically-based scheme for the urban energy budget in atmospheric models. *Boundary-Layer Meteorol.*, **94,** 357–397
Mills, G. M. and Arnfield, A. J.	1993	Simulation of the energy budget of an urban canyon—II. Comparison of the model results with measurements. *Atmos. Environ.*, **27B,** 171–181
Nunez, M. and Oke, T. R.	1977	The energy balance of an urban canyon. *J. Appl. Meteorol.*, **16,** 11–19
Oke, T. R.	1981	Canyon geometry and the nocturnal heat island: Comparison of scale and field observations *J. Climatol.*, **1,** 237–254
	1982	The energetic basis of the urban heat island. *Q. J. R. Meteorol. Soc.*, **108,** 1–24
	1987	*Boundary layer climates*, 2nd edn. Routledge, UK
Oke, T. R. and East, C.	1971	The urban boundary layer in Montreal. *Boundary-Layer Meteorol.*, **1,** 411–437
Oke, T. R., Johnson, G. T., Steyn, D. G. and Watson, I. D.	1991	Simulation of surface urban heat islands under 'ideal' conditions at night. Part 2: Diagnosis of causation. *Boundary-Layer Meteorol.*, **56,** 339–358
Oke, T. R., Sproken-Smith, R. A., Jáuregui, E. and Grimmond, C. S. B.	1999	The energy balance of central Mexico City during the dry season. *Atmos. Environ.*, **33,** 3919–3930
Owczarek, S.	1997	Vector model for calculation of solar radiation intensity and sums incident on tilted surfaces. Identification for the three sky condition in Warsaw. *Renew. Energ.*, **11,** 77–96
Rotach, M. W.	1999	On the influence of the urban roughness sublayer on turbulence and dispersion. *Atmos. Environ.*, **33,** 4001–4008
Schmid, H. P., Cleugh, H. A., Grimmond, C. S. B. and Oke, T. R.	1991	Spatial variability of energy fluxes in suburban terrain. *Boundary-Layer Meteorol.*, **54,** 249–276
Smirnova, T. G., Brown, J. M. and Benjamin, S. G.	1997	Performance of different soil model configurations in simulating ground surface temperatures and surface fluxes. *Mon. Weather Rev.*, **125,** 1870–1884
Voogt, J. A. and Grimmond, C. S. B.	2000	Modeling surface sensible heat flux using surface radiative temperatures in a simple urban area. *J. Appl. Meteorol.*, **39,** 1679–1699